Published in final edited form as:
Blood Cells Mol Dis. 2009 ; 43(2): 202–210. doi:10.1016/j.bcmd.2009.04.001.

Microarray analysis of prothrombin knockdown in zebrafish

Kenneth R. Day and **Pudur Jagadeeswaran**†
Department of Cellular and Structural Biology, The University of Texas Health Science Center at San Antonio, San Antonio, TX 78229 And Department of Biological Sciences, University of North Texas, Denton, TX. 76203

Abstract

The serine protease thrombin is generated from its precursor, prothrombin, in the coagulation cascade and plays a central role in fibrin deposition and platelet activation mediated through the protease activated receptors. Knockdown of prothrombin in the zebrafish was previously shown to recapitulate the phenotype observed in prothrombin knockout mice, such as an absence of blood pericardial edema, and hemorrhage. However, the role of thrombin during embryogenesis is not fully understood. To find genes affected by potential thrombin signaling in embryogenesis before blood circulation microarray analysis was performed using total RNA prepared from antisense-injected, knockdown embryos versus mismatch-injected at 20 hours post fertilization. A total of 63 upregulated and downregulated genes were identified with duplicate microarrays using dye reversal and a two-fold difference limitation. Real time RT-PCR for 10 selected genes identified by the microarray confirmed the expression changes in these genes. One particular gene, phlda3, was at least eleven fold upregulated, and in situ hybridization revealed expansion of phlda3 expression in the central nervous system, branchial arches, and head endoderm in knockdown embryos. The identification of these genes regulated by thrombin according to microarray analysis should provide a greater understanding of the effects of thrombin activity in the early vertebrate embryo.

Keywords

zebrafish; prothrombin; morpholino; embryonic development

Introduction

Thrombin is the central serine protease of the blood coagulation cascade that converts fibrinogen to fibrin and is generated from its zymogen precursor prothrombin by the action of Xa. Thrombin also mediates a cellular response primarily through cleavage and activation of the G-protein-coupled, protease activated receptor-1 (PAR-1) that has been extensively characterized in platelet activation [1]. In addition to being a potent platelet agonist, thrombin also exerts activity in fibroblasts, smooth muscle, neurons, endothelium and other cell types [1–5].

Targeted gene inactivation of prothrombin in mice leads to embryonic lethality at approximately midgestation [6–8]. A prothrombin-deficient phenotype exhibited many

†Address correspondence to: Pudur Jagadeeswaran, Ph.D., Department of Biological Sciences, University of North Texas, Denton, TX. 76203, Phone: (940) 565-3601, FAX: (210) 565-3821, Jag@unt.edu.

developmental defects related to yolk sac vascular integrity such as enlarged and dilated capillary structure, vessels devoid of blood, and flattening of visceral yolk sac endoderm. In the zebrafish, knockdown of prothrombin produced an early phenotype in which greater than one third of all embryos have abnormalities in their overall growth with defects in the anterior and posterior regions [9]. When grown to 48 hours post fertilization (hpf), these embryos recapitulated the prothrombin deficient phenotype observed in the mouse embryo. They exhibited an absence or reduced number of blood cells, reduced blood flow, pericardial edema, and blood clots in the trunk region. These results showed a conserved role for thrombin in vertebrate embryonic development.

To elucidate changes in gene expression affected by prothrombin knockdown, hybridizations on microarrays consisting of oligonucleotides representing 14,000 genes were performed using RNAs made from 20 hpf antisense morpholino-injected (ASMO) embryos displaying the previously characterized abnormalities versus mismatch control-injected (MMMO) embryos. Hybridization results revealed a total of 63 upregulated and downregulated genes using a twofold expression change limit. Real time quantitative RT-PCR (QRTPCR) was used to confirm microarray results for 10 genes identified. A gene that was 11-fold upregulated, called phlda3, encodes a small protein containing a pleckstrin homology domain that could be involved in regulating IP_3 release, recruitment of proteins to the intracellular membrane surface, and membrane shape changes. Phlda3 was shown to be upregulated in the CNS with possible expansion of expression in the branchial arches and anterior endoderm. Additionally, the sry-related HMG box transcription factor, sox21, was shown to be downregulated greater than twofold. Sox21 is duplicated in the zebrafish genome and is termed as sox21a or sox21b [10]. Sox21a is expressed throughout the forebrain, midbrain and hindbrain, but shows greatest expression in the midbrain-hindbrain boundary (MHB) [11]. Reduction of sox21a MHB expression in knockdown embryos further verified microarray results. All of these results taken together indicate a potential role for thrombin signaling in the embryonic brain. The identification of sox21a, phlda3, and the other genes regulated by thrombin according to microarray analysis will provide a greater understanding of the effects of thrombin activity in the early vertebrate embryo.

Materials and methods

Morpholino Oligonucleotides and Microinjections of Zebrafish Embryos

A prothrombin antisense morpholino oligonucleotide, 5′ GTTTGGCTCCCATCCTTGAGAGTGA-3′ (ASMO) against the 5′-UTR to target the translational start site of the zebrafish prothrombin mRNA and a control oligonucleotide 5′ GTTTCGCTCGCATGCTTCAGACTGA-3′ (MMMO) with 5 base mismatches (mismatches indicated by underlines) were purchased from Gene-Tools LLC, Philomath, OR. Embryos were microinjected with 4.5 nL ASMO (1 mg/mL) or MMMO diluted in Danieau buffer into the yolk of one to four cell stage embryos [12]. Injected embryos were maintained in embryo medium at 28°C until 20 hpf. Embryos that exhibited early phenotype (depicted in Fig. 1) as previously reported were collected [9].

Oligonucleotide microarray experiments

Total RNA was isolated from 20 hpf embryos collected from 4 independent microinjection experiments. The first batch of RNA was made from 16 embryos (each embryo was injected with 4.5ng ASMO) displaying the early phenotype, and 16 embryos injected with 4.5 ng MMMO that were normal in appearance. The same selection procedure was used for 3 more experiments using 12 embryos each for ASMO and MMMO groups. Total RNA was isolated from embryos, and independent RNA preparations were pooled, run through columns provided

in the RNeasy® Mini Kit (Qiagen Inc., Valencia, CA), and final RNA integrity, purity, and concentration were again estimated by UV spectrophotometry and gel electrophoresis.

The University of Texas Southwestern Medical Center at Dallas Microarray Core Facility performed the following steps using the high quality total RNA prepared. Five micrograms of pooled ASMO and MMMO RNAs were used with the Superscript II Reverse Transcriptase kit (Invitrogen, Carlsbad, CA) for first strand cDNA synthesis. Second strand was synthesized using the SuperScript™ Double-Stranded cDNA Synthesis Kit (Invitrogen). Reactions were incubated at 16°C for 2h, then 1 μl T4 polymerase was added, incubated for 10 min at 16°C, and finally reactions were stopped by adding 10 μl of 0.5M EDTA to inhibit all enzymes.

Complementary DNA was purified using the GeneChip Sample Cleanup Module (Affymetrix, Santa Clara, CA) according to the protocol supplied by the manufacturer. Antisense RNA (aRNA) was amplified by T7 in vitro transcription using the MessageAmp aRNA Kit (Ambion, Austin, TX) with unlabeled NTPs, 16 μl cDNA, and incubated at 37°C overnight according to protocol. The GeneChip Sample Cleanup Module (Affymetrix) was then used again for aRNA purification, and aRNA was quantified by spectrophotomety. Probes were labeled using the ASAP RNA Labeling Kit (Perkin Elmer, Boston, MA) in two separate reactions using 2μg of each aRNA with ASAP Cyanine-3 Reagent or ASAP Cyanine-5 Reagent according to protocol. Each labeled probe was then combined, mixed into the same tube, and purified using a Microcon YM-30 filter column. RNA probe synthesis was also repeated by reverse labeling ASMO and MMMO RNA samples.

Five microliters of probe were then mixed with preheated ASAP Hybridization buffer (Perkin Elmer) and placed on to two Zebrafish 14K arrays (MWG Biotech Inc., High Point, NC) with each array being divided into two slides (array A and array B) each representing 14,067 total genes. Probes containing the MMMO-Cy3 and ASMO-Cy5 mixtures were used for two microarray A slides and the reverse label mixture (MMMO-Cy5 and ASMO-Cy3) was used for two microarray B slides for performing the hybridizations in duplicate. Probes were hybridized for 14–16h at 62°C. Slides were then washed, dried, and scanned for data acquisition using a GenePix® 4000B scanner (Axon Instruments, Inc., Union City, CA).

Oligonucleotide microarray data processing

Scanned GenePix data was imported into the online GeneTraffic™ DUO two-color microarray data analysis software version 2.8–9 (Iobion Informatics LLC, La Jolla, CA) for data analysis. LOWESS sub-grid normalization was used for each slide, and background was automatically subtracted from a generated correction value. Two fold change criteria were used to select differentially expressed genes from the microarray to complete an annotated list of results with fold level changes greater than or equal to 2-fold or less than or equal to 0.5-fold. Data was sorted by selection of successful hybridizations. All genes were manually grouped according to function or subcellular localization.

Real time RT-PCR

Total RNA was made from early phenotype and MMMO-injected reference embryos at 20hpf similar to RNAs prepared for the microarray as described below. Three independent RNA preparations were made from a pool of embryos for each ASMO and MMMO-injected group by homogenization in RNAzol™ B Isolation of RNA solution (Leedo Medical Laboratories, Houston, TX) using a Brinkman polytron homogenizer. RNA pellets were resuspended in nuclease-free water at 60°C for 10 min. RNAs were treated with DNAse using the DNA-*free*™ DNase Treatment kit (Ambion, Austin, TX) at 37°C for 30 min to eliminate any potentially contaminating genomic DNA, and 500 ng of treated total RNA were used for cDNA

synthesis using Taqman® Reverse Transcription Reagents (Applied Biosystems, Foster City, CA) according to protocol.

Primers were designed online with Primer3 (http://frodo.wi.mit.edu/cgi-bin/primer3/primer3.cgi/). All primer sequences used for validation experiments are reported in Table 2, and were used with β-actin primers: forward 5′ TTCTGGTCGGTACTACTGGTATTGTG 3′, and reverse 5′ ATCTTCATCAGGTAGTCTGTCAGGT 3′. Primers used for the detailed confirmation to specifically detect sox21a and b duplicated genes in their expression in knockdown embryos were: 5′ CCGCATTATTCCGTGCTC 3′ and 5′ ATGCCAGGTAAGGTTCATGC 3′ for sox21a; 5′ AAGGACAAATTCGCGTTCC 3′ and 5′ TGAGGCGTAGGAGAAAGACG 3′ for sox21b. Each real time PCR reaction was performed in triplicate using β-actin as the control for normalization. Primers were diluted to.5 pmoles/μl in a forward and reverse primer mix, and 10.5 μl primer were mixed with 12.5 μl 2X SYBR® Green PCR Master Mix (Applied Biosystems) and 2 μl cDNA for each developmental stage containing a 25μl reaction volume in a 96 well format (Applied Biosystems). Reactions were performed using the ABI Prism 7900 HT Sequence Detection System with cycling parameters that were 95°C for 10 min, followed by 40 cycles of 95°C for 15 s and 60°C for 1 min. Raw data was analyzed and exported using the ABI prism SDS 2.0 software. Dissociation curves were also recorded to verify a single product was amplified for each primer set.

Raw fluorescent data was imported into the automated calculation workbook entitled Data Analysis for Real-Time PCR (DART-PCR) designed by Peirson, Butler, and Foster [13] that enables the rapid calculation of threshold cycle, amplification efficiency, and resulting R_0 values. Results for each target gene were then normalized against β-actin to determine a fold expression value. Each reaction in triplicate was repeated in 3 experiments using independent RNA preparations.

Whole mount in situ hybridization

Partial cDNAs for phlda3 and sox21a were amplified by RT-PCR and cloned into the pCR® II-TOPO® vector. The primers containing sequences 5′ GACGGGTATCTGGAGAAGAGG 3′ and 5′ CTGTTCCTGCCGGTCTGA 3′ were used for phlda3. Sox21 primer sequences were used previously as reported in [10]. Antisense probes were transcribed from linearized vector using a MEGAscript™ Sp6 high yield transcription kit (Ambion Inc., Austin, TX) with each reaction containing a 3:1 ratio of Digoxigenin-11-UTP (Roche Diagnostics Corporation Indianapolis, IN) to UTP.

ASMO and MMMO embryos were prepared, prehybridized, and hybridized overnight at 70° C as previously reported [14]. Embryos were washed to remove probe and blocked in blocking solution (2mg/mL BSA, 5% sheep serum, 1% DMSO in PBT, pH 7.4) for 4h and then incubated overnight at 4°C with Anti-Digoxigenin-AP Fab fragments (Roche Diagnostics Corporation Indianapolis, IN) diluted 1:4500 in blocking solution. Embryos were washed extensively to remove unbound antibody, equilibrated in NTMT buffer (.1M Tris pH 9.5,.1M NaCl,.05 M $MgCl_2$,.1% Tween 20), and stained in NBT/BCIP solution (Roche Diagnostics Corporation). Reactions were stopped by PBT washes, dehydrated in methanol as done previously and stored until clearing in 2:1 benzyl benzoate/benzyl alcohol. Images were then under captured under bright field using a Nikon CoolPix 995 CCD camera mounted on a Nikon Optiphot microscope using 2X and 10X objectives.

Results

Genes affected by prothrombin knockdown during embryonic development before initiation of blood circulation

To identify prospective genes affected by thrombin signaling in the zebrafish embryo, pooled total embryonic RNAs from three separate microinjection experiments at 20 hpf were used for probe labeling and microarray analysis using a 14K zebrafish array. Only ASMO embryos that exhibited posterior abnormalities with a reduction of the yolk sac extension as reported previously were used for RNA extraction along with MMMO embryos at the same stage (Fig. 1). Hybridizations were performed on duplicate slides using the same sample and were referred to as array 1 and 2. Following corrections for background intensity and normalization between filters, an overall intensity distribution for the ratio of expression for each representative gene was constructed by plotting log ratio intensity of ASMO versus MMMO. These plots revealed that the overall distributions for array 1 and 2 duplicates were similar, and verified that independent hybridizations gave comparable normalized intensity values (Fig. 2). There were relatively few genes expressed above the 2-fold ratio and below the 0.5-fold ratio as indicated by red or green colored outliers. A 2-fold change criterion was then used to obtain a gene list that excluded flagged data. The majority of genes affected by prothrombin knockdown were found with both of the hybridizations performed. According to both arrays, 35 total represented genes were upregulated with 27 of them being confirmed in duplicate, and 28 were downregulated with 23 in duplicate. All of these genes were classified according to cellular localization, function, or structure (Table 1). The greatest number of genes affected was related to metabolism and mitochondria (19% of total genes affected), while only a single ligand and transcription factor gene were affected in their expression. Cell structure and motility comprised 17% of genes affected, but contained different isoforms for similar genes such as keratin and parvalbumin. Some of the genes on the array such as for an unknown cysteine protease, the alpha globins, a putative membrane protein, the heat shock protein 90-beta, annexin max 3, and smd2 were spotted more than once which gave multiple values that were similar for each array.

Validation of gene expression changes affected by prothrombin knockdown

Microarray findings were then validated by QRTPCR by selection of 5 upregulated and downregulated genes with priority given to greatest fold level change. Zebrafish genomic DNA sequence information for each of these genes was obtained by using the accession number provided with each spot identity. Primers were designed from zebrafish gene sequence reported on the array. Table 2 shows primer sequences used for microarray validation. Individual amplification curves demonstrated significant differences in gene expression in comparison to β-actin controls in which no change was detected between ASMO and MMMO embryos. Raw fluorescent data was used to analyze reaction efficiency and R_0 values were generated to obtain a fold level change value relative to MMMO embryos after normalization using β-actin controls according to the DART procedure [13]. QRTPCR results indicated a confirmation of trends in the changes of these selected genes with respect to their upregulation or downregulation as shown by each microarray (Fig. 3).

Interestingly, one particular gene reported on the microarray as bwr1c is also named IPL. BLAST results using mouse bwr1c/IPL sequence against the zebrafish genome gave greatest percent identity for another gene called phlda3. Both IPL and phlda3 belong to members of a pleckstrin homology-related gene family [15]. We could distinguish that the gene affected as shown by microarray and QRTPCR was indeed phlda3 and not IPL in the zebrafish by synteny (Fig. 4A). The cluster of genes flanking phlda3 is arranged similar in human, but there is an inversion when compared to zebrafish and mouse. QRTPCR using phlda3 gene specific primers showed greater upregulation for phlda3 than the microarray (Fig. 3). To further confirm

this result, semi-quantitative RTPCR using an alternative phlda3 primer set to amplify a larger sized product was performed to visualize product intensity by agarose gel electrophoresis compared to an another control that previously showed no difference in expression between ASMO and MMMO embryos. Results indicated that phlda3 is highly upregulated in knockdown embryos (Fig. 4B). This corroborated the fact that phlda3 is the gene that is altered in its expression shown by microarray and QRTPCR.

Similar to difficulties in discerning between phlda3 and IPL in the zebrafish, gene duplication was noted for sox21 in the zebrafish genome. The duplicate genes were designated as sox21a and sox21b [10]. Since the primer set designed for confirmation by QRTPCR could amplify both sox21 isoforms, two more primer sets were designed specifically to amplify sox21a and sox21b by QRTPCR. Results revealed a greater downregulation of sox21b compared to sox21a when normalized to β-actin controls in reference to MMMO embryos, with both indicating an approximate 2-fold repression or greater (Fig. 4C). To further validate this data, two additional primer sets were designed to amplify a greater sized product that also gave results indicating a decrease in expression between ASMO and MMMO embryos for sox21a and sox21b, but with a greater reduction in sox21b (Fig. 4D). Control reactions using β-actin specific primers showed no difference in expression between the two groups.

The PCR products for phlda3 and sox21a were amplified (Figure 4B and 4D) and cloned for probe synthesis. In situ hybridization analysis revealed an expansion of phlda3 expression in the central nervous system particularly in the forebrain, midbrain, endoderm of the head, and the branchial arches (compare Fig. 5A,B and 5C,D). Interestingly, there also appeared to be abnormal upregulated expression in the tail region that was not observed in the mismatch control that showed a segmented pattern (compare Fig. 5B and 5D). It was also noted from phlda3 expression that furrow formation that occurred at the MHB appeared to be absent in the knockdown embryos along with the upregulation. A decrease in sox21a expression was found in the MHB of ASMO embryos compared to controls (compare Fig. 5E,F and 5G,H). Comparison of lateral views between ASMO and MMMO embryos showed that some MHB expression was lost in ASMO embryos (Fig. 5E and 5G). It was apparent from dorsal views that there was also a lack of furrow formation at the MHB along with the preservation of characteristic sox21a patterning, albeit with the reduction of expression at the MHB (Fig. 5F and 5H).

Discussion

This study used a method to understand gene expression changes in prothrombin knockdown embryos using total RNA extracted from embryos and not from specific tissues or cell types. Elucidation of the greatest differences in gene expression was advantageous because it found potential genes controlled by thrombin in the entire embryo compared to approaches in which only tissue or cell type specific genes would be isolated. Since use of embryonic total RNA revealed a small number of relatively large changes in gene expression, minute changes in gene expression that may be vital to developmental processes may have been undetected. However, this method is currently used to find basic transcriptional programs in development induced by single factors with the use of mutant zebrafish embryos [16]. This approach was also used for zebrafish embryos treated under hypoxic conditions as well as for retinoid deficient rat embryos [17,18]. The use of total embryonic RNAs for microarray analysis also gave a manageable number of genes that allows microarray validation by QRTPCR possible for every gene identified. This technique may also be used to gain a broader understanding of the basis for embryonic lethality caused by prothrombin gene inactivation. The zebrafish system is beneficial for direct observation of prothrombin knockdown phenotype, which resembles the knockout phenotype [9] and facilitates analysis of gene expression by preparing total RNA from the affected embryos.

A total of 63 genes were revealed by both microarrays with 50 of these genes being confirmed in duplicate over a total of 14,000 genes represented. It is known that thrombin may upregulate collagen synthesis in platelets, fibroblasts, hepatic stellate cells, mesangial cells, and vascular smooth muscle. Thrombin signaling may further amplify signaling events as an autocrine mediator during vascular injury, cell signaling, or in the process of wound healing [19–22]. Collagen Ia2 downregulation as well changes in the expression of other structural components, such as claudin e and keratin, suggests a role for thrombin stimulation or regulation of extracellular events in embryonic growth.

After microarray validation, it is apparent that phlda3 (pleckstrin homology like domain family A, member 3) is the most significantly affected gene. It is approximately 4-fold upregulated by microarray analysis, and 11-fold upregulated according to QRTPCR. This discrepancy may be due to cross-hybridization of closely related family members such as with Ipl (Imprinted in Placenta and Liver) or TGAG51 (T-cell Death Associated Gene 51) which also contain pleckstrin homology (PH) domains, and indicates that precaution should be taken with the interpretation of oligo-based arrays if array construction did not take into account the presence of other highly related sequences used to represent each zebrafish gene. Multiple methods of confirmation such as synteny analysis between zebrafish and mammalian genes, and in situ hybridization provided validation in addition to spatial and temporal information.

Phlda3 is a very small protein; the central PH domain contains 100 amino acids out of a total size of 125 amino acids. It has moderate affinity for membrane phosphatidylinositol phophate binding, and PH-domain dependent accumulation at membrane ruffles [23]. Phlda3 is expressed ubiquitously in mouse fetal tissues except for liver [15], while Ipl is specifically expressed in extraembryonic tissues, i.e., the visceral yolk sac endoderm, embryonic liver, and kidney [15,24]. Knockout of Ipl results in overgrowth and expansion of the spongiotrophoblast layer while gene deletion of phlda3 had no effect [25]. Although it is difficult to discern the function of phlda3 in embryonic development, it could possess a redundant function in mammals based upon knockout studies, but may have a specific role in zebrafish. Thrombin signaling could possibly regulate phlda3 to prevent G protein- induced, cytoskeletal and membrane shape responses in certain cells [15,26,27] since it has been shown previously that PH domain phosphorylation appears to inhibit Gβγ-activated PI3K by interacting with Gβγ [28–30]. However, phlda3 gene regulation by subsequent thrombin activation of its receptor in cells remains to be determined.

The only transcription factor identified in our studies was sox21. After validation by independent primers for sox21a and b, it is evident that both may be affected. This observation indicates that precaution should be taken in consideration of duplicated genes. Sox21 is a part of the group B Sox proteins, belongs to the HMG box superfamily, and has been described as a repressor of neuronal differentiation and causes neurite retraction [31]. Sox21a expression controlled by potential thrombin activity could be a mechanism by which neurite outgrowth is regulated in embryonic development since thrombin plays a substantial role in neurite retraction [32–34], but this also requires further investigation.

The reduction of expression observed in the MHB of knockdown embryos provides a new avenue to be explored for the mechanism of thrombin action in the embryonic brain before the initiation of blood circulation. Thrombin is known to signal through PARs expressed on neuronal cells [2,4,35–38]. All of these data taken together with the known roles for phlda3, sox21, thrombin activity on neuronal cells, and their coexpression in the CNS suggest a potential model for thrombin activity in the developing vertebrate brain.

The microarray approach used here may provide insight into potential downstream transcriptional activity induced by thrombin signaling in early vertebrate embryogenesis in

processes such as cell growth, differentiation, and migration. The genes elucidated here may possess unknown roles in response to thrombin activity that are unique during embryogenesis.

Acknowledgments

This study was supported by National Institutes of Health Grant to P.J.

References

1. Coughlin SR. Thrombin signalling and protease-activated receptors. Nature 2000;407:258–64. [PubMed: 11001069]
2. Wang H, Reiser G. Thrombin signaling in the brain: the role of protease-activated receptors. Biol Chem 2003;384:193–202. [PubMed: 12675511]
3. Chang MC, Chan CP, Wu HL, Chen RS, Lan WH, Chen YJ, Jeng JH. Thrombin-stimulated growth, clustering, and collagen lattice contraction of human gingival fibroblasts is associated with its protease activity. J Periodontol 2001;72:303–13. [PubMed: 11327057]
4. Suidan HS, Niclou SP, Monard D. The thrombin receptor in the nervous system. Semin Thromb Hemost 1996;22:125–33. [PubMed: 8807708]
5. Kataoka H, Hamilton JR, McKemy DD, Camerer E, Zheng YW, Cheng A, Griffin C, Coughlin SR. Protease-activated receptors 1 and 4 mediate thrombin signaling in endothelial cells. Blood 2003;102:3224–31. [PubMed: 12869501]
6. Degen JL. Genetic interactions between the coagulation and fibrinolytic systems. Thromb Haemost 2001;86:130–7. [PubMed: 11486998]
7. Sun WY, Witte DP, Degen JL, Colbert MC, Burkart MC, Holmback K, Xiao Q, Bugge TH, Degen SJ. Prothrombin deficiency results in embryonic and neonatal lethality in mice. Proc Natl Acad Sci U S A 1998;95:7597–602. [PubMed: 9636195]
8. Xue J, Wu Q, Westfield LA, Tuley EA, Lu D, Zhang Q, Shim K, Zheng X, Sadler JE. Incomplete embryonic lethality and fatal neonatal hemorrhage caused by prothrombin deficiency in mice. Proc Natl Acad Sci U S A 1998;95 :7603–7. [PubMed: 9636196]
9. Day K, Krishnegowda N, Jagadeeswaran P. Knockdown of prothrombin in zebrafish. Blood Cells Mol Dis 2004;32:191–8. [PubMed: 14757435]
10. Argenton F, Giudici S, Deflorian G, Cimbro S, Cotelli F, Beltrame M. Ectopic expression and knockdown of a zebrafish sox21 reveal its role as a transcriptional repressor in early development. Mech Dev 2004;121:131–42. [PubMed: 15037315]
11. De Martino SP, Errington F, Ashworth A, Jowett T, Austin CA. sox30: a novel zebrafish sox gene expressed in a restricted manner at the midbrain-hindbrain boundary during neurogenesis. Dev Genes Evol 1999;209:357–62. [PubMed: 10370117]
12. Gregory M, Hanumanthaiah R, Jagadeeswaran P. Genetic analysis of hemostasis and thrombosis using vascular occlusion. Blood Cells Mol Dis 2002;29:286–95. [PubMed: 12547218]
13. Peirson SN, Butler JN, Foster RG. Experimental validation of novel and conventional approaches to quantitative real-time PCR data analysis. Nucleic Acids Res 2003;31:e73. [PubMed: 12853650]
14. Jowett T. Double in situ hybridization techniques in zebrafish. Methods 2001;23:345–58. [PubMed: 11316436]
15. Frank D, Mendelsohn CL, Ciccone E, Svensson K, Ohlsson R, Tycko B. A novel pleckstrin homology-related gene family defined by Ipl/Tssc3, TDAG51, and Tih1: tissue-specific expression, chromosomal location, and parental imprinting. Mamm Genome 1999;10:1150–9. [PubMed: 10594239]
16. Qian F, Zhen F, Ong C, Jin SW, Meng Soo H, Stainier DY, Lin S, Peng J, Wen Z. Microarray analysis of zebrafish cloche mutant using amplified cDNA and identification of potential downstream target genes. Dev Dyn 2005;233:1163–72. [PubMed: 15937927]
17. Ton C, Stamatiou D, Liew CC. Gene expression profile of zebrafish exposed to hypoxia during development. Physiol Genomics 2003;13:97–106. [PubMed: 12700360]

18. Flentke GR, Baker MW, Docterman KE, Power S, Lough J, Smith. Microarray analysis of retinoid-dependent gene activity during rat embryogenesis: increased collagen fibril production in a model of retinoid insufficiency. Dev Dyn 2004;229:886–98. [PubMed: 15042712]
19. Dabbagh K, Laurent GJ, McAnulty RJ, Chambers RC. Thrombin stimulates smooth muscle cell procollagen synthesis and mRNA levels via a PAR-1 mediated mechanism. Thromb Haemost 1998;79:405–9. [PubMed: 9493599]
20. Fiorucci S, Antonelli E, Distrutti E, Severino B, Fiorentina R, Baldoni M, Caliendo G, Santagada V, Morelli A, Cirino G. PAR1 antagonism protects against experimental liver fibrosis. Role of proteinase receptors in stellate cell activation. Hepatology 2004;39:365–75. [PubMed: 14767989]
21. Gaca MD, Zhou X, Benyon RC. Regulation of hepatic stellate cell proliferation and collagen synthesis by proteinase-activated receptors. J Hepatol 2002;36:362–9. [PubMed: 11867180]
22. Kaizuka M, Yamabe H, Osawa H, Okumura K, Fujimoto N. Thrombin stimulates synthesis of type IV collagen and tissue inhibitor of metalloproteinases-1 by cultured human mesangial cells. J Am Soc Nephrol 1999;10:1516–23. [PubMed: 10405207]
23. Saxena A, Morozov P, Frank D, Musalo R, Lemmon MA, Skolnik EY, Tycko B. Phosphoinositide binding by the pleckstrin homology domains of Ipl and Tih1. J Biol Chem 2002;277:49935–44. [PubMed: 12374806]
24. Saxena A, Frank D, Panichkul P, Van den Veyver IB, Tycko B, Thaker H. The product of the imprinted gene IPL marks human villous cytotrophoblast and is lost in complete hydatidiform mole. Placenta 2003;24:835–42. [PubMed: 13129680]
25. Frank D, Fortino W, Clark L, Musalo R, Wang W, Saxena A, Li CM, Reik W, Ludwig T, Tycko B. Placental overgrowth in mice lacking the imprinted gene Ipl. Proc Natl Acad Sci U S A 2002;99:7490–5. [PubMed: 12032310]
26. Majumdar M, Seasholtz TM, Buckmaster C, Toksoz D, Brown JH. A rho exchange factor mediates thrombin and Galpha(12)-induced cytoskeletal responses. J Biol Chem 1999;274:26815–21. [PubMed: 10480888]
27. Klarlund JK, Guilherme A, Holik JJ, Virbasius JV, Chawla A, Czech MP. Signaling by phosphoinositide-3,4,5-trisphosphate through proteins containing pleckstrin and Sec7 homology domains. Science 1997;275:1927–30. [PubMed: 9072969]
28. Colman, RW., et al. Hemostasis and thrombosis: basic principles and clinical practice. Vol. 4. Philadelphia: Lippincott Williams & Wilkins; 2001.
29. Abrams CS, Zhang J, Downes CP, Tang X, Zhao W, Rittenhouse SE. Phosphopleckstrin inhibits gbetagamma-activable platelet phosphatidylinositol-4,5-bisphosphate 3-kinase. J Biol Chem 1996;271:25192–7. [PubMed: 8810277]
30. Abrams CS, Zhao W, Brass LF. A site of interaction between pleckstrin's PH domains and G beta gamma. Biochim Biophys Acta 1996;1314:233–8. [PubMed: 8982277]
31. Ohba H, Chiyoda T, Endo E, Yano M, Hayakawa Y, Sakaguchi M, Darnell RB, Okano HJ, Okano H. Sox21 is a repressor of neuronal differentiation and is antagonized by YB-1. Neurosci Lett 2004;358:157–60. [PubMed: 15039105]
32. Fritsche J, Reber BF, Schindelholz B, Bandtlow CE. Differential cytoskeletal changes during growth cone collapse in response to hSema III and thrombin. Mol Cell Neurosci 1999;14:398–418. [PubMed: 10588393]
33. Gill JS, Pitts K, Rusnak FM, Owen WG, Windebank AJ. Thrombin induced inhibition of neurite outgrowth from dorsal root ganglion neurons. Brain Res 1998;797:321–7. [PubMed: 9666159]
34. Gurwitz D, Cunningham DD. Thrombin modulates and reverses neuroblastoma neurite outgrowth. Proc Natl Acad Sci U S A 1988;85:3440–4. [PubMed: 2835773]
35. Turgeon VL, Houenou LJ. The role of thrombin-like (serine) proteases in the development, plasticity and pathology of the nervous system. Brain Res Brain Res Rev 1997;25:85–95. [PubMed: 9370052]
36. Turgeon VL, Lloyd ED, Wang S, Festoff BW, Houenou LJ. Thrombin perturbs neurite outgrowth and induces apoptotic cell death in enriched chick spinal motoneuron cultures through caspase activation. J Neurosci 1998;18:6882–91. [PubMed: 9712658]
37. Turgeon VL, Salman N, Houenou LJ. Thrombin: a neuronal cell modulator. Thromb Res 2000;99:417–27. [PubMed: 10973669]

38. Suidan HS, Stone SR, Hemmings BA, Monard D. Thrombin causes neurite retraction in neuronal cells through activation of cell surface receptors. Neuron 1992;8:363–75. [PubMed: 1310864]

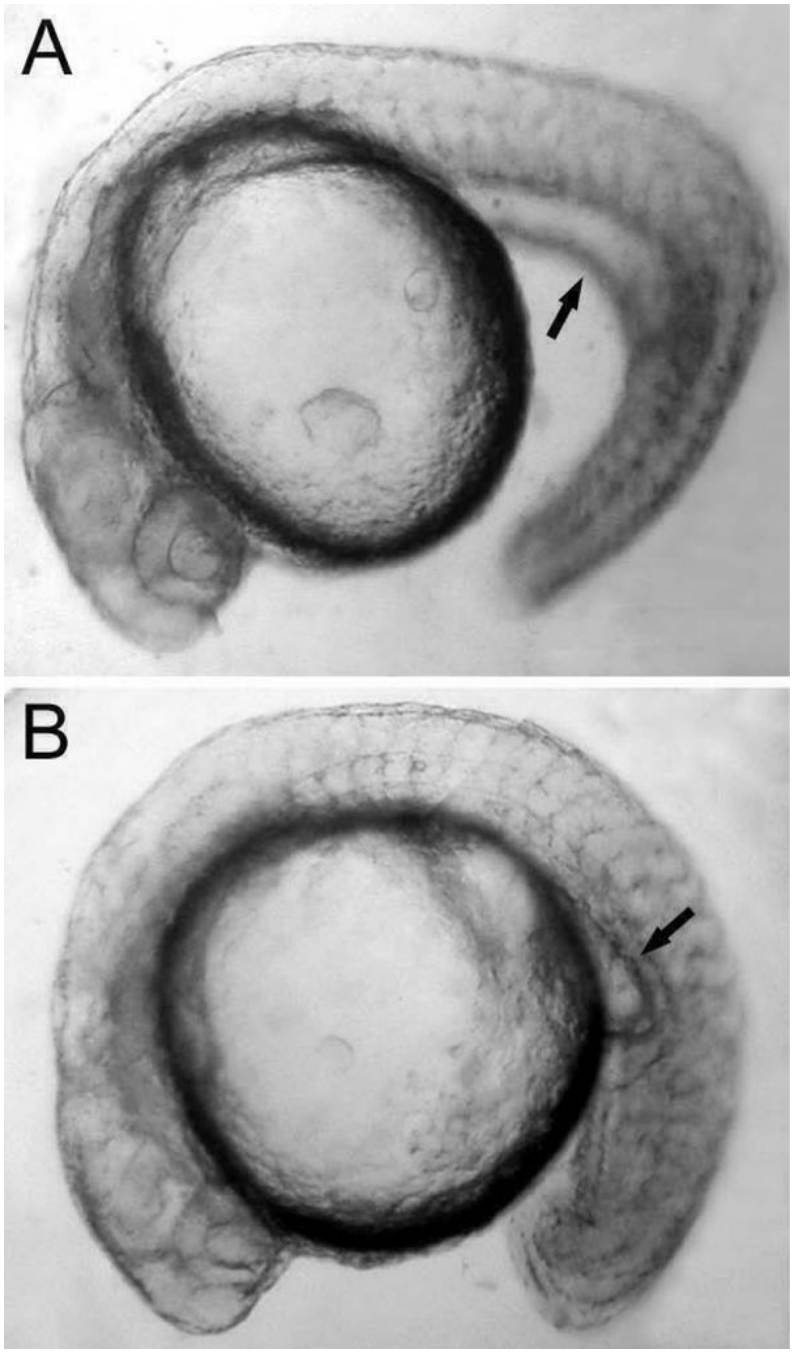

Fig. 1.

Overall gross appearance of zebrafish embryos grown to 20 hpf after microinjection of morpholinos. Compared to the mismatch-injected control (**A**), there is aberrancy in the trunk and tail with a large reduction in the yolk sac extension (indicated by arrows) in the antisense injected-knockdown (**B**). All antisense embryos exhibiting this phenotype were selected for RNA preparation for microarray analysis.

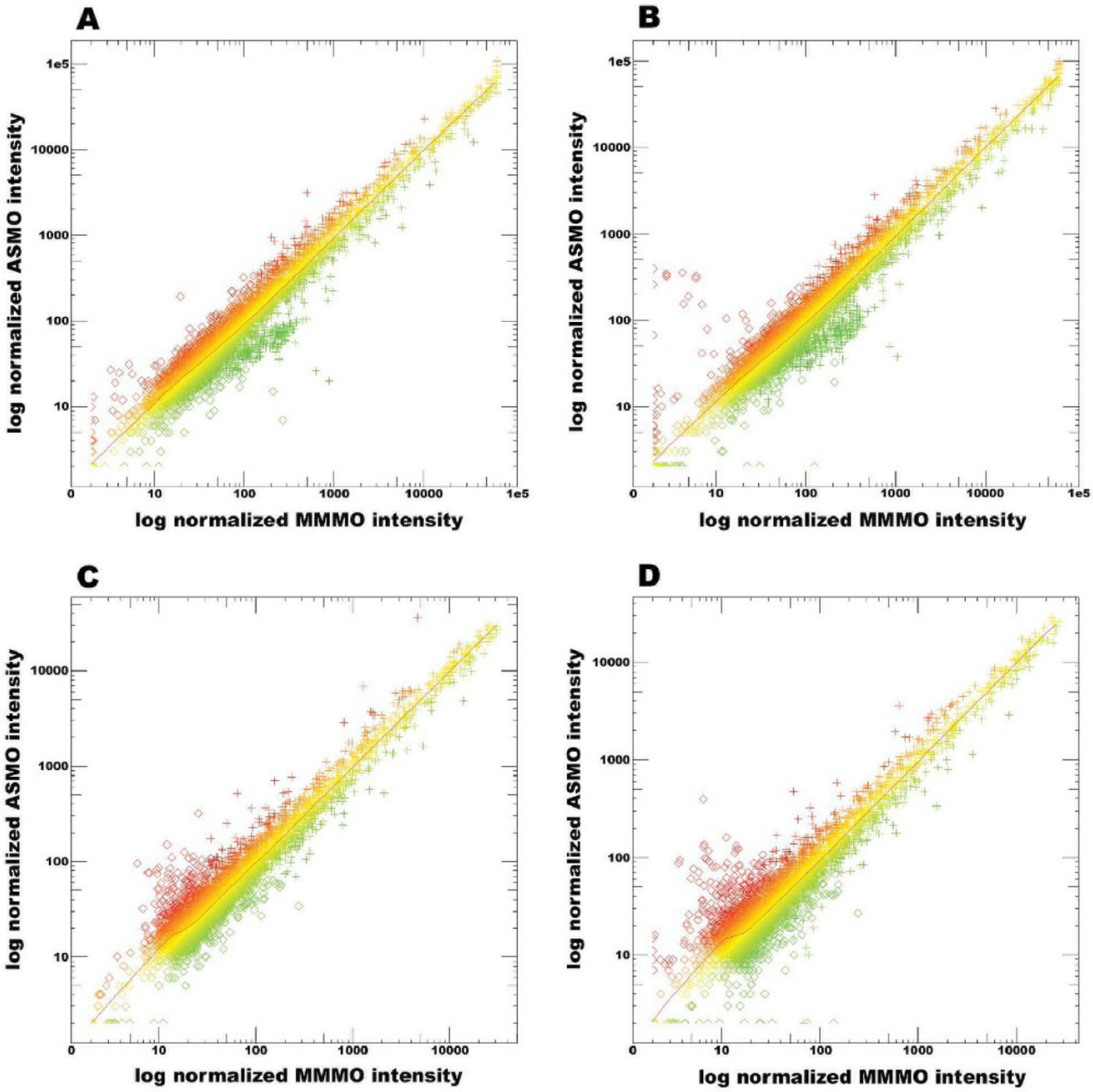

Fig. 2.

Distribution of microarray data following normalization. Distribution of duplicate hybridizations showing average normalized ratio signal intensities for microarray 1 (**A and C**) and microarray 2 (**B and D**). Red color indicates upregulated genes above 2-fold and green color represents genes downregulated below 2-fold. Plotted lines indicate a ratio of 1 between the two groups. Diamonds represent flagged data not included in the analysis.

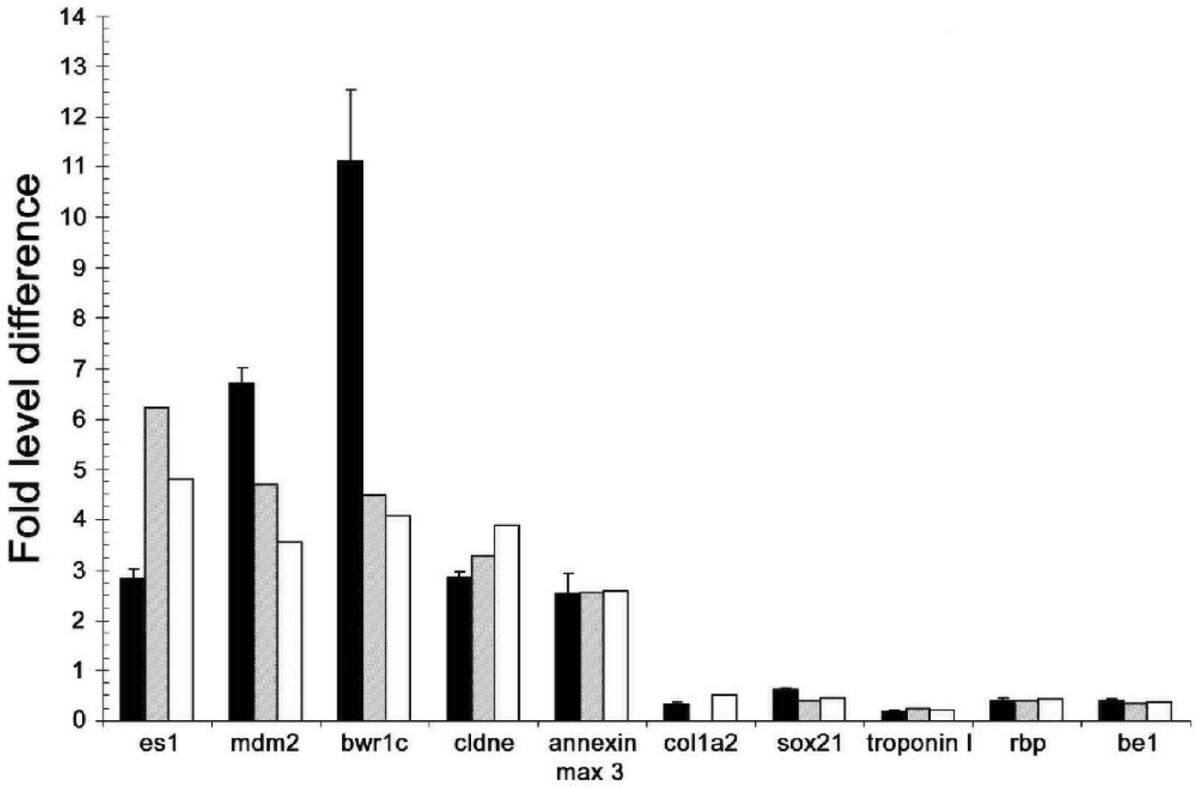

Fig. 3.

Real time RT-PCR confirmation results for 10 selected genes from the microarray. The bar graphs show the average fold level difference for real time RT-PCR in black compared to microarray 1 levels shown in grey and microarray 2 in white. All RT-PCR results are normalized to β-actin controls. Error bars indicate S.E.M.

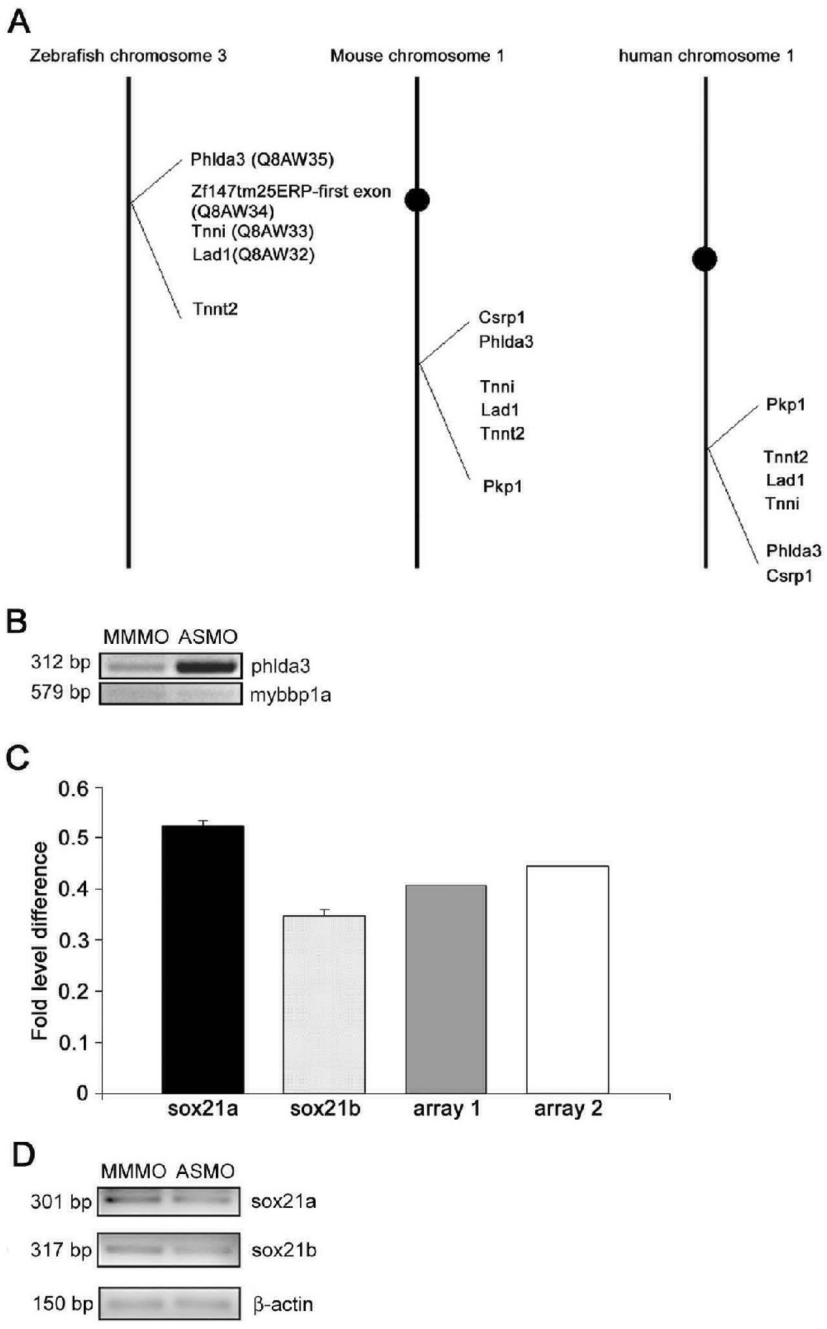

Fig. 4.

Detailed validation of phlda3 and sox21 gene expression differences. Bwr1c identity on the microarray is actually phlda3 as shown by synteny. Phlda3 gene location is similar among zebrafish, mouse, and human chromosomes (**A)**. RT-PCR using an alternative phlda3 primer set with a control reaction for a gene that showed no difference between groups (**B**). Real time RT-PCR confirmation results using sox21a and sox21b specific primer sets in ASMO injected embryos (black and light grey bars, respectively) and corresponding fold changes for sox21 indicated by each microarray (dark grey and white bars) (**C**). Results are normalized to β-actin controls and error bars show S.E.M. Semi-quantitative RT-PCR using another set of sox21a and b specific primers (**D**). Lanes containing reactions with MMMO or ASMO embryo RNA

are indicated at the top of each lane, and β-actin control reactions are shown in the bottom panel.

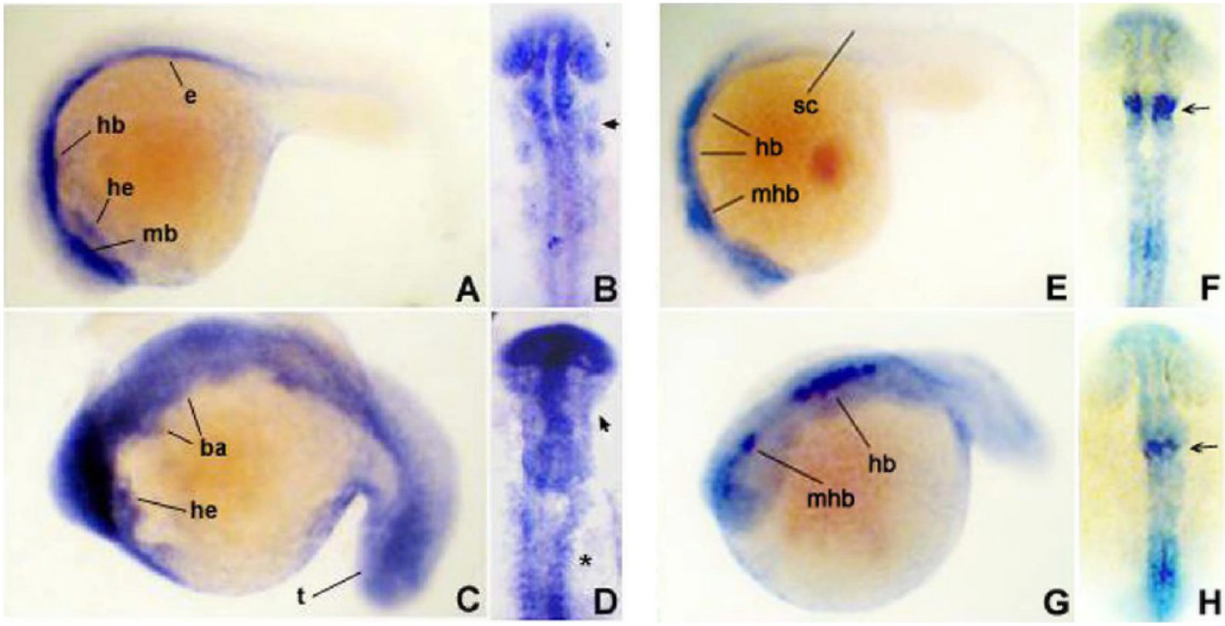

Fig. 5.

In situ hybridization for phlda3 and sox21a at 20 hours post-fertilization. The overall normal expression of phlda3 shown in MMMO-injected embryos (**A** and **B**) is upregulated and expanded in prothrombin knockdown embryos (**C** and **D**). Lateral views are shown in **A** and **C**, and dorsal views in **B** and **D**. Arrowheads indicate branchial arches in which there may an expansion of expression in knockdown embryos along with head endoderm (**B vs. D**). Asterisk indicates an expansion of phlda3 expression in the tail that is not normally observed in control embryos that appeared to have a segmented pattern. Sox21a was normally expressed in the optic stalks, the MHB, and faintly in the ventral hindbrain and spinal cord as shown by a lateral view of an MMMO-injected control embryo (**E**). Missing expression was found primarily in the MHB of knockdown embryos with fainter expression in the anterior region of the ventral hindbrain in which there appears to be a gap between the MHB and the posterior region of the ventral hindbrain when compared to controls (**E vs. G**). Dorsal views also show a reduction of MHB expression as depicted by arrows in addition to an apparent lack of furrow formation at the site of MHB expression in knockdown embryos compared to the MMMO (**F vs.H**). ba, branchial arches; e, endoderm; he, head endoderm; hb, hindbrain; mb, midbrain; mhb, midbrain hindbrain boundary; sc, spinal cord; t, tail.

TABLE 1

Identities of Genes Affected by Prothrombin Knockdown[a]

Gene Description[b]	Accession No.	Fold-Change ASMO/MMMO Array 1	Fold-Change ASMO/MMMO Array 2
Cell cycle			
murine double minute 2 homolog; mdm2 - danio rerio	NM_131364	4.69	3.55
putative helicase ruvbl - homo sapiens	AF218313	2.66	
cyclin g1 - homo sapiens	L49504	8.08	8.82
Cell environment, communication			
chaperonin 60; hsp60 - rattus norvegicus	U68562	2.85	2.2
heat shock cognate;hsc70 - danio rerio	L77146	2.22	2.19
heat shock protein 90-beta; hsp90beta - danio rerio	AF042108	2.22, 2.01	2.14, 2.07
heavy-chain binding protein bip - xenopus laevis	U62807	2	
Globins			
embryonic alpha-type globin - oncorhynchus mykiss	AB015448	0.405, 0.332	0.436 0.341
embryonic 1 beta-globin (be1); be1 - danio rerio	NM_131759	0.339	0.371
alpha globin type-3 - cyprinus carpio	AB063102	0.370, 0.303, 0.348	0.341, 0.366, 0.316
Ligand			
jagged3; jag3 - danio rerio	NM_131863	0.215	0.236
Membrane associated, receptors			
annexin max3 - oryzias latipes	Y11254	2.6, 2.51	2.62, 2.58
p17-beckwith-wiedemann region 1 c; bwr1c - homo sapiens	AF035444	4.47	4.06
ser/thr protein kinase par-1a - homo sapiens	AF387637		0.490
homolog to liprin-beta1 putative - mus musculus	AK014559	0.303	0.295
bone morphogenetic protein receptor, type 1b; bmpr1b - danio rerio	NM_131457	0.289	0.302
mhc class i protein zr2; zr2 - cyprinus carpio	AJ007849	0.472	0.447
Metabolism, mitochondria			
mitochondrial phosphate transporter precursor - rattus norvegicus	M23984	2.13	2.03
hes1 - homo sapiens	Y07572	6.23	4.79
atp synthase beta-subunit - cyprinus carpio	AB023582	2.53	2.57
16.7kd protein - homo sapiens	BC015639	2.23	2.11
cytochrome c oxidase subunit vib aa 1–86 - bos Taurus	X15112	0.288	0.310
cytochrome c oxidase subunit i; cox1 - danio rerio	AC024175	3.5	3.32
glycolate oxidase - mus musculus	AF104312	0.476	0.49
nadh dehydrogenase subunit 3; nd3 - danio rerio	AC024175	0.46	0.480
phosphoglycerate mutase; pgam2 - homo sapiens	M55674	0.356	0.457
pyruvate kinase l - homo sapiens	D13243	0.360	0.316
omega class glutathione-s-transferase - takifugu rubripes	AF325922	2.94	3.16
retinol binding protein; rbp - danio rerio	NM_130920	0.398	0.430
Other			
tartrate-resistant acid phosphatase type 5 - rattus sp.	M76110	2.12	2
nucleoside diphosphate kinase-z2; ndpk-z2 - danio rerio	AF202053	0.447	
oocyte-type fatty-acid binding protein - danio rerio	AF448057	0.496	
ard-1 n-acetyltransferase homologue; te2 - mus musculus	AF133093	2.31	2.33
Protease			
cysteine proteinase - cyprinus carpio	L30111	2.11, 2.46	2.07, 2.36
Protein turnover			
polyubiquitin - xenopus laevis	M11512	2.08	
polyubiquitin - bos Taurus	Z18245	2.11	
alpha 4 subunit of 20s proteasome - carassius auratus	AB027707	2.17	2.28
26s proteasome subunit p40.5 - homo sapiens	AF107837	2.33	2.31
Ribosome, translation			
lysyl-trna synthetase; kars - mus musculus	AF328904	2.1	2.14
ribosomal protein s27 - rattus rattus	X59375	5.28	5.62
putative similar to 60s ribosomal protein l22 heparin binding protein			

Gene Description[b]	Accession No.	Fold-Change ASMO/MMMO Array 1	Fold-Change ASMO/MMMO Array 2

TABLE 2

Primers Used in Microarray Confirmation[a]

Gene identified	Forward Primer	Reverse Primer	Size (bp)
es1	t a c g a a g c c t a t g t g g a c g a g	t t c a g g t g t t t g t g g t c t g g	164
mdm2	a g a a c c c t g c g t c a t c t g t c	c a a g g c a a c t c c c a a a c t t c	225
bwr1c	c c a c t c t g g a t t g t g t g g a g	g t g a c a a a t g c c t g t t c c t g	183
cldne	a g a g c a c g g g a c a g a t g c	g g c g a t g g a c a c t t t a g c c	191
annexin max3	g c c t t c c a g c t c a a a t a t g c	a g g g c a t t c c t g a a g t c t c c	182
col1a2	g a t g g c a a c a a t g g c a g a c	g a a g a c c a c g a c c a c c t c t c	226
sox21	g a g t t c a g a g g c g g a a g a t g	g t a a t c c g g g t g c t c c t t c	167
troponin I	g a t g c t t c a g g c t c t g c t g	c t t t c t g c c a c c c a t a c c a g	154
rbp	g a t a a c t a c g c a a t c c a c t a c t c g	g c a g c c t c a c a g a a a c c a g	196
be1	g c c a c c t a t g c t g a t t t g a g	t c t t c c c a g a g c g g a c a c	167

[a] All primers were designed from zebrafish genomic DNA exon sequence derived from BLAST results between Genbank sequence obtained from accession numbers reported for microarray spot indentity and ENSEMBL zebrafish genome database.